AN AUTOMATED RAYLEIGH WAVE DETECTION ALGORITHM

Eric P. Chael
Sandia National Laboratories
Albuquerque, NM 87185

Sponsored by DOE

Abstract

The desire to operate denser networks in order to monitor seismic activity at lower thresholds leads to greater emphasis on automated data processing. An algorithm for detecting and characterizing long-period Rayleigh wave arrivals has been developed and tested. The routine continuously monitors all directions of approach to a station, in a manner similar to beamforming. The detector is based on cross-powers between the Hilbert-transformed vertical and rotated horizontal signals, so it is sensitive to both the power and polarization properties of the three-component wavefield. Elliptically polarized Rayleigh arrivals are enhanced, while linearly polarized Love waves and body phases are suppressed. A test using one month of data from station ANMO demonstrated that this technique can with high reliability detect Rayleigh arrivals which would be visible to an analyst. The measured arrival times and azimuths are accurate enough to permit automated association of the detections to events in a bulletin.

Key words: detection, Rayleigh wave, surface wave, long period, automated data processing, polarization

Objective:

Effective verification of a Comprehensive Test Ban will require an extensive seismic network capable of monitoring at a fairly low magnitude threshold. Such a network will generate a large quantity of waveform data and record hundreds or even thousands of events daily. The resulting data analysis burden will force an increased reliance on automated processing. Current networks routinely process short-period (SP) waveforms by computer to automatically detect and associate body arrivals, and then locate the events. Improvements to these routines are necessary in order to improve their reliability. In contrast, the analysis of long-period (LP) waveforms, important for event identification via the M_S:m_b discriminant, remains a largely manual process. First-generation algorithms for automated LP processing have only recently become available. One approach to this problem, currently being tested by the prototype International Data Center under GSETT-3, is to examine the LP signals for the existence of surface waves from known events. An alternate approach, which has been developed and tested for this report, is to continuously scan the LP data for surface arrivals from anywhere. Detected arrivals can then be associated to existing event solutions, or used to help constrain the solutions for events which produce few SP detections.

The Rayleigh detection algorithm discussed here exploits the elliptical polarization of Rayleigh arrivals both to enhance detection sensitivity over that achieved from vertical signals alone, and to decrease the sensitivity to unwanted body or Love arrivals. Several authors have developed algorithms for polarization analysis of seismic waves. Some of these (*e.g.*, Simons, 1988; Samson, 1977) have required knowledge of event location, so that the radial and transverse directions are known *a priori*. Others (*e.g.*, Samson and Olson, 1981) have relied on continuously tracking the dominant polarization direction, in essence dynamically rotating the waveforms to this continually changing azimuth. The method addressed in this work seeks to continuously and independently monitor all directions for Rayleigh arrivals. The technique is comparable to beamforming done for seismic arrays, in which beams are pointed in several different directions then separately scanned for arrivals. Simultaneously watching all directions should offer signal-to-noise improvement compared to tracking only the current dominant direction.

Research Accomplished:

An automated Rayleigh wave detection routine has been designed, and its performance tested using one month of LP data. Three-component long-period or broadband waveforms are required for the Rayleigh detection algorithm. The first step in the processing is to detrend and then bandpass filter the signals. A third-order Butterworth filter with a passband of 0.01 to 0.06 Hz has produced good results. Next, the vertical signal is Hilbert transformed using a 255-point FIR filter (Stearns and David, 1988). This has the effect of phase shifting the vertical waveform by 90°, which converts the elliptical polarization of Rayleigh waves into linear motion. A beneficial side effect of this operation is to change linearly polarized body waves to elliptical polarization, which will de-emphasize them in subsequent processing. At each time step, the 3-by-3 data covariance matrix is calculated over a specified window length. A duration of 80 s has been used for this short-term-average (STA) window, equivalent to 4 cycles at the dominant Rayleigh period near 20 s. The covariance matrix at each time step is then rotated over azimuth from 0° to 85° in 5°

increments. At each azimuth step, the two covariance elements which represent the cross-powers between the vertical and each of the rotated horizontals are extracted. These are used as the STA estimates for the two orthogonal azimuths corresponding to the angle of rotation (0° to 85°) and the direction 90° clockwise from this (90° to 175°). It is not necessary to calculate the covariances for azimuths of 180° to 355°, since the values would simply be the negative of those for 0° to 175°. A strong positive STA response indicates Rayleigh energy with the appropriate retrograde elliptical motion arriving from the specified direction. Using the cross-power between the vertical and horizontal motions should improve the signal-to-noise by about a factor of two (3 dB), compared to using the power on either axis alone. Long-term-averages (LTAs) of each of the STAs are updated at each time step. A recursive scheme was used for the LTA computations, providing exponential weighting of past STAs. The time constant for this weighting was set at 800 s.

A detection function is produced for each look direction by calculating a weighted STA/LTA ratio versus time. Alternatively, one can view the result as a detection surface with an altitude that varies as a function of both azimuth and time. Two weights are applied to the STA/LTA ratios of the cross-powers. The first of these weights is the absolute value of the correlation coefficient between the vertical and the radial signal for a given azimuth. Because the vertical has been Hilbert transformed, it should be well correlated with the horizontal when a Rayleigh wave is arriving from the specified direction. The second weight is based on the relative amplitudes of the vertical and radial components. Its purpose is to emphasize arrivals whose Z and R motions are similar in amplitude. Both of these weights are readily calculated from the elements of the rotated covariance matrix. The detection surface is scanned for peaks exceeding a threshold altitude. When a detection is made, the peak's onset time, amplitude and central azimuth are recorded, along with the peak amplitude of the vertical signal following the detection. The entire Rayleigh detection algorithm was implemented in MATLAB, so it can be easily modified to test different processing details. The current routine should be able to process full-period LP data (1 sps) from roughly 100 stations on a single Pentium-class PC.

Figure 1(a) shows 20 min of LP data from station COL near Fairbanks, AK for an earthquake in the Aleutians. The horizontal components have been rotated to the radial (middle trace) and transverse (bottom trace) directions. A strong Rayleigh wave arrives near 600 s on the LPZ and LPR traces. The LPT signal shows a strong Love arrival near 400 s, with coda extending into the Rayleigh window. This coda contaminates a standard polarization analysis of the Rayleigh wave. Figure 1(b) displays the detection surface produced by these records; the surface is shown for azimuths of 180° to 360°, where the data produce a positive peak. The Rayleigh wave produced a very strong peak at the proper time and azimuth for this event. Note that the large Love arrival had little effect on the surface. The Love coda caused the ridge running to the left from the peak, but did not significantly bias the peak's location. Figure 2(a) shows a much weaker Rayleigh arrival at station ANMO (Albuquerque, NM) from an event in the South Pacific. For this plot the traces were bandpass filtered between 0.01 Hz and 0.06 Hz to enhance the arrival. Again the horizontals have been rotated to radial and transverse, and the Rayleigh wave begins just prior to 600 s. The resulting detection surface in Figure 2(b) shows a prominent peak at the Rayleigh onset time, centered near the correct backazimuth to the event. This peak jumps abruptly from the preceding terrain, despite the relatively low SNR of the arrival on the seismograms. A second

peak occurs near 900 s on the plot, caused by the resurgence in the Rayleigh coda which can be seen on the LPZ trace.

To test the performance of the detection algorithm in routine operation, I processed all of the ANMO data for the month of October, 1993. The resulting detection log was compared to the NEIC event bulletin for this month. A total of 192 detections were reported, of which 157 could be attributed to 108 different events in the bulletin. For those events which caused multiple detections, the trigger corresponding to the Rayleigh onset could usually be readily determined from its time and azimuth. Multiple detections for an event were usually due to fluctuations in the Rayleigh coda, overtone energy preceding the Rayleigh, or S arrivals. Errors in the estimated backazimuths for identified Rayleigh arrivals had a mean of 0° and a standard deviation of 15°. Thus the backazimuth measurements are sufficiently accurate to assist automated association of Rayleigh detections with events. Figure 3 shows the performance of the detector as a function of event magnitude and distance, for all events which had M_S values in the NEIC bulletin. Solid circles represent events which produced Rayleigh detections by the algorithm, open circles events which did not. This plot indicates that the routine can detect Rayleigh waves from most events with M_S over 4 to distances of 30°, with the sensitivity gradually decreasing to an M_S of about 5 at the furthest ranges. The undetected large events at a distance of 108° were aftershocks in the coda of larger events. Adjusting the LTA time constant or changing the logic for ending a previous detection may yield better performance in such cases.

Conclusions and Recommendations:

An algorithm for detecting Rayleigh surface wave arrivals on three-component long-period records has been developed and tested. The routine continuously monitors all directions of approach to a station, in a manner analogous to array beamforming. The detector's response is sensitive to both the power and polarization properties of the wavefield, so that Rayleigh waves are preferentially enhanced over other arrivals. A one-month test of the algorithm with station ANMO demonstrated that it can reliably detect an overwhelming majority of the Rayleigh waves visible on the seismograms, and the detection time and azimuth measures are sufficiently accurate for reliable association to bulletin events.

Further work is needed in three areas. First, estimates of arrival amplitude and period need to be refined, in order to enable accurate automated M_S measurements. Second, better methods for screening non-Rayleigh detections should be developed and tested. Examining a detection's frequency content may be useful here. Finally, more testing is needed to establish the performance for regional events ($\Delta < 30°$), which will become of increasing importance under a CTBT.

References:

Samson, J. C. (1977). Matrix and Stokes vector representations of detectors for polarized waveforms: theory, with some applications to teleseismic waves, *Geophys. J. R. astr. Soc.* **51**, 583-603.

Samson, J. C. and J. V. Olson (1981). Data-adaptive polarization filters for multichannel geophysical data, *Geophysics* **46**, 1423-1431.

Simons, R. S. (1968). A surface wave particle motion discrimination process, *Bull. Seism. Soc. Am.* **58**, 629-637.

Stearns, S. D. and R. A. David (1988). *Signal Processing Algorithms*, Prentice-Hall, Inc., Englewood Cliffs, NJ.

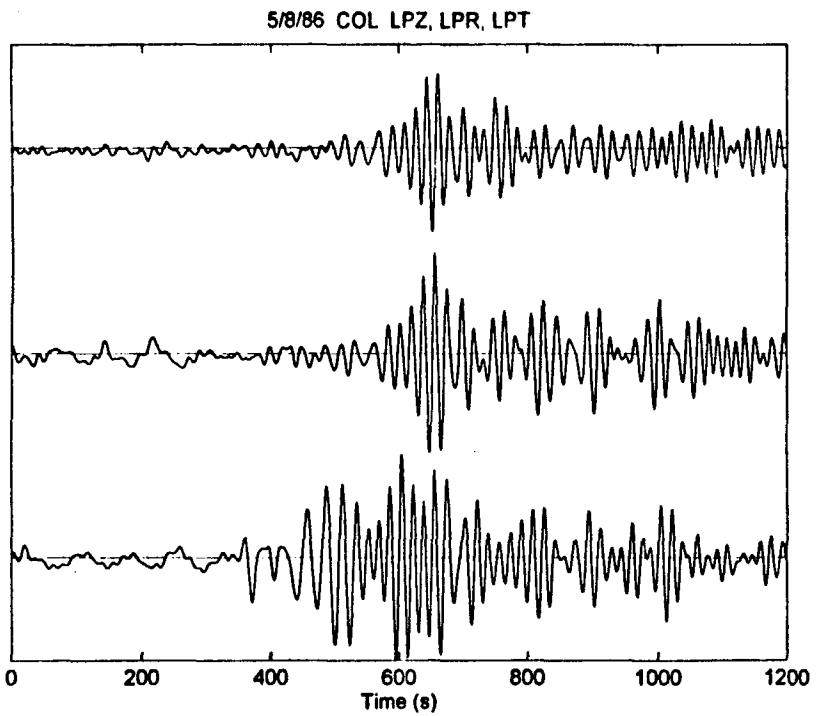

(a)

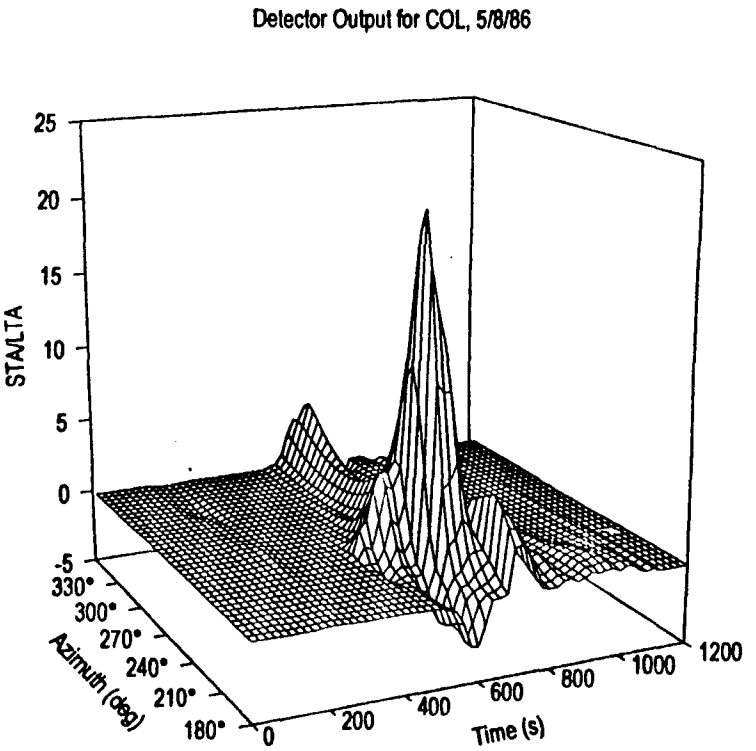

(b)

Figure 1. (a) Vertical, radial and transverse records from station COL of an M_S 5.4 earthquake in the Aleutian Islands on May 8, 1986, at a distance of 20° and a backazimuth of 241°. (b) Output of the detection algorithm for the signals shown in (a).

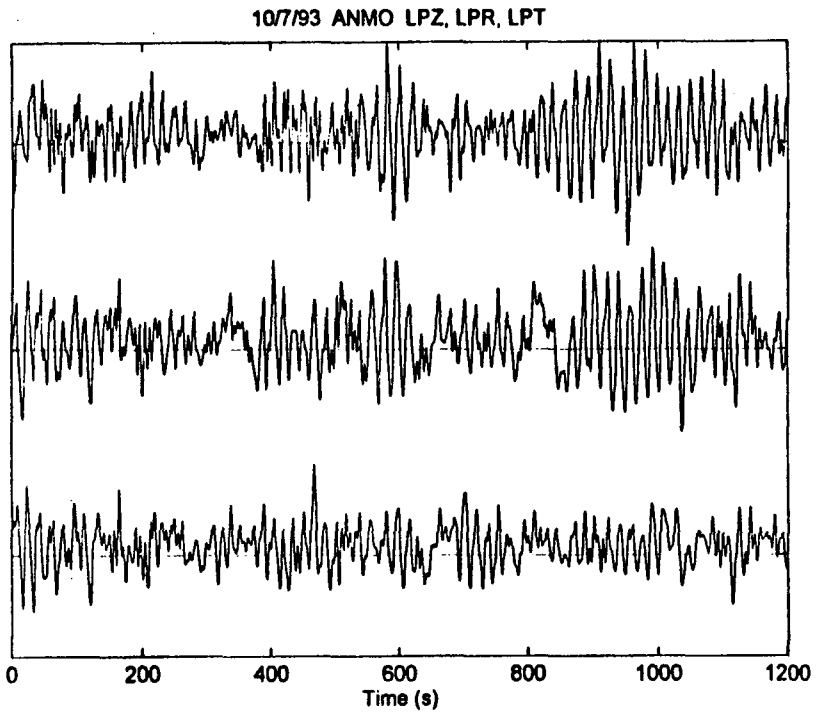

(a)

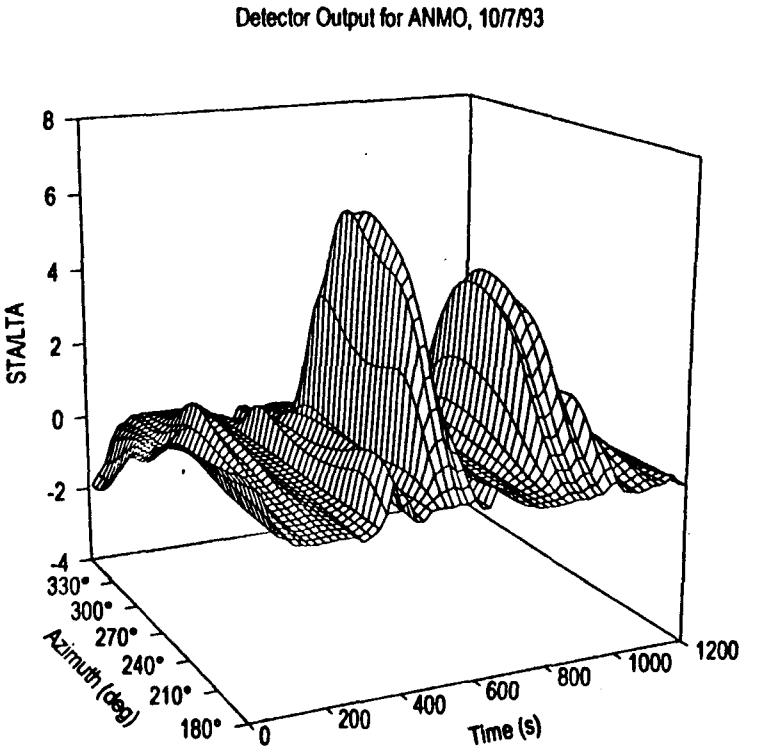

(b)

Figure 2. (a) Vertical, radial and transverse records from station ANMO of an M_S 4.3 earthquake in the South Pacific on October 7, 1993, at a distance of 97° and a backazimuth of 232°. (b) Output of the detection algorithm for the signals shown in (a).

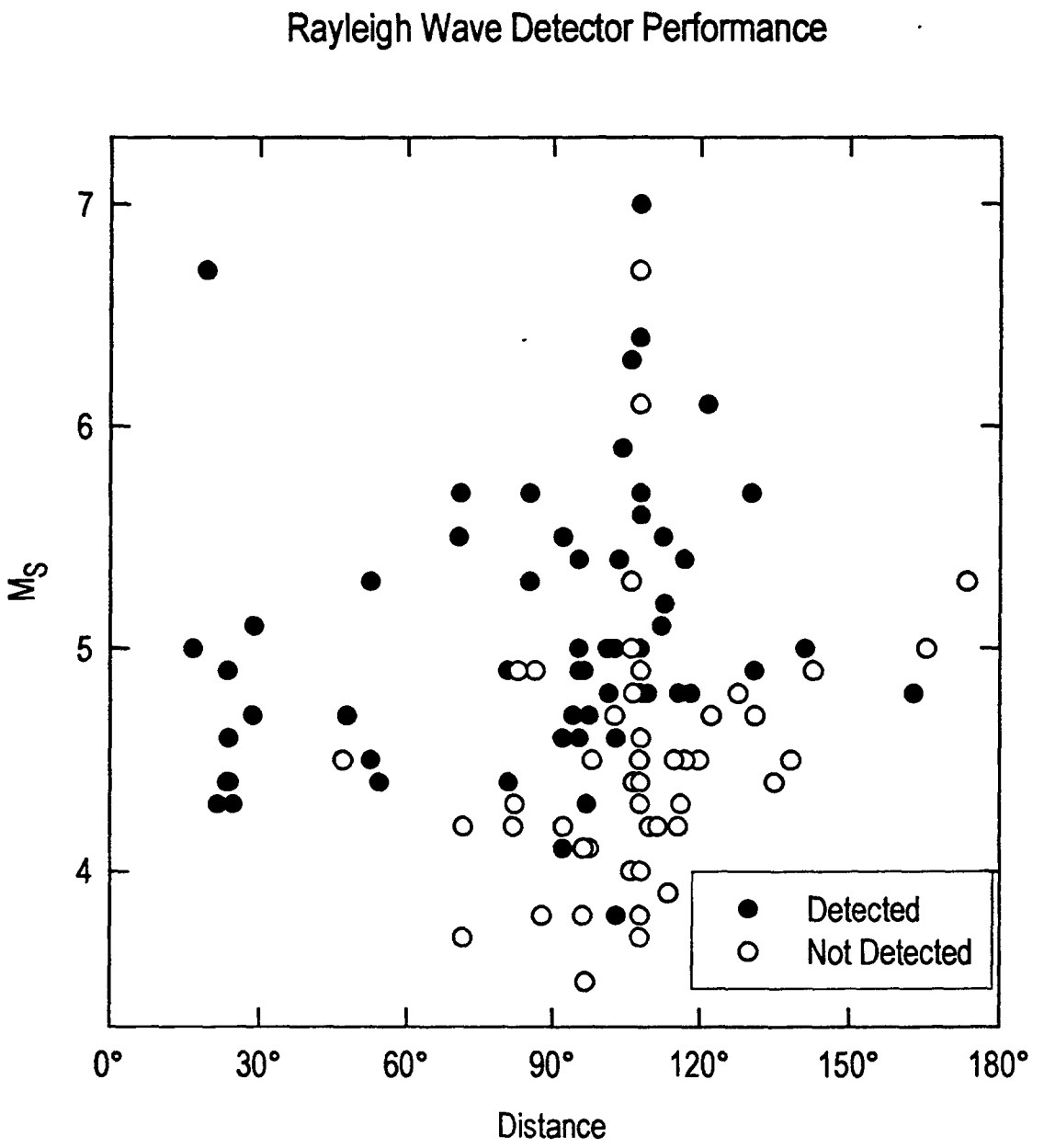

Figure 3. Detector performance as a function of event distance and surface wave magnitude. Solid circles represent events whose Rayleigh waves were detected by the algorithm, open circles indicate that a Rayleigh arrival was not detected.